Available online at www.sciencedirect.com
SCIENCE DIRECT
Polymer 47 (2006) 2448–2454
polymer
www.elsevier.com/locate/polymer

Ultrasonic measurement of orientation in HDPE/*i*PP blends obtained by dynamic packing injection molding

Bobing He, Xue Yuan, Hong Yang, Hong Tan, Lingxi Qian, Qin Zhang, Qiang Fu *

State Key Laboratory of Polymer Materials Engineering, Department of Polymer Science and Materials, Sichuan University, Chengdu 610065, China

Received 21 September 2005; received in revised form 28 December 2005; accepted 9 February 2006

Abstract

The orientation of polymer chain has a great effect on its mechanical properties, therefore, it is always an important issue on how to characterize, accurately and quickly, the orientation of polymer chain during processing. In this article, according to the property that ultrasound travels in different velocities in anisotropic media, normal incident shear wave was utilized to explore the orientation structure of HDPE/*i*PP blends obtained by dynamic packing injection molding. The ultrasonic technique is consistent with the 2D-WAXS in charactering the orientation degree of polymer chains, although ultrasonic technique focuses on the overall orientation of polymer blends while the 2D-WAXS reveals the crystalline orientation of each component. Our work demonstrates that ultrasonic technique might be a reliable, fast and easy way to characterize the orientation structure of crystalline polymer blends. The ultrasonic measurements were performed off-line, but the achievement provides the possibility for on-line detection of orientation structure in injection molding by using ultrasonic technique.

Keywords: Polymer blends; Orientation; Shear wave

1. Introduction

Generally, the mechanical properties of polymer are far inferior to their theoretical values when polymer chain arrayed at random [1,2]. However, they can be greatly improved by enhancing the orientation of polymer chain. Therefore, it is always an important issue on how to characterize the orientation of polymer chain quickly and conveniently. Up to now, a variety of methods have been developed to explore the orientation structure on-line or off-line, including 2D-WAXS [3–9], 2D-SAXS [3–5,10], optical birefringence [11–13], IR dichroism [14–17], Raman and Infrared spectroscopy [18] et al. These conventional methods can well determine the orientation structure off-line, but they have rarely been applied to on-line detection during processing, especially in injection molding, partly due to certain technique difficulties. Although many methods can be utilized to determine the orientation of polymer chain, different results and phenomena may occur due to different principle based. Additionally, every method has its own limitation and can only be used in some special cases. For example, optical birefringence method is good for highly oriented fiber but not good for low oriented injection molded samples; spectroscopy method needs complicated calibration and X-ray method is very good for crystalline polymers but not for amorphous polymers.

Ultrasonic technique, as a novel method to characterize orientation structure using normal incident shear wave, has many advantages, like non-invasion, convenience, extremely quick feedback, and strong sensitivity to anisotropic structure, which make ultrasonic technique quite suitable for real-time detection. Edwards et al. [19] demonstrated a technique using a normal incident shear wave transducer to measure the orientation in injection molded low density polyethylene (LDPE). They observed that the shear wave traveled in different velocities with respect to the particle displacement direction. That is, the velocity with particle displacement parallel to orientation direction was higher than that vertical to orientation direction, and large difference in velocity indicated a high orientation. They also investigated the orientation variation of LDPE during injection molding with the transducer mounted on the mold. However, the real-time detection of polymer orientation during injection molding still remains a challenge task, mainly due to the very short solidification time by this processing method.

In recent years, dynamic packing injection molding has been found to be a very important way to control polymer

* Corresponding author. Tel.: +86 28 854 60953; fax: +86 28 854 05402.
E-mail address: qiangfu@scu.edu.cn (Q. Fu).

0032-3861/$ - see front matter © 2006 Elsevier Ltd. All rights reserved.
doi:10.1016/j.polymer.2006.02.020

morphology, particularly, the chain orientation [20–22]. As a part of long-term project aimed at real-time detection of polymer orientation during injection molding, we are seeking to establish a fundamental understanding of processing–orientation–ultrasonic velocity relationships. In this work, we first prepared HDPE/*i*PP blends via dynamic packing injection molding (DPIM), in which the specimen was forced to move repeatedly in a chamber by two pistons that moved reversibly with the same frequency as the solidification progressively occurred from the mold wall to the molding core. In this way, highly oriented samples can be obtained. Our novel point is the highly oriented structure of polymer obtained by dynamic packing injection molding, which makes the ultrasound signal much stronger and more reliable. Edwards et al. used tensile property to verify the ultrasound data and some conflicts between the ultrasound data and tensile strength was mentioned in Ref. [19]. In our work, since PP and HDPE are crystalline, 2D-WAXS was preferentially chosen for comparison, and the consistency of the ultrasound data with 2D-WAXS was observed. Our result shows that the ultrasonic velocity difference between in parallel along and vertical to shear flow direction can be used to characterize the whole orientation in the blends.

2. Experimental

2.1. Materials and sample preparation

*i*PP and HDPE used in the experiment are commercial products. *i*PP purchased from Duzisan Ltd Co. has a melt flow index (MFI) of 3 g/10 min and a density of 0.91 g/cm^3. HDPE was obtained from Yansan Petrochemical Co., whose MFI is 15 g/10 min and density is 0.968 g/cm^3. Melt blending was conducted using TSSJ-25 co-rotating twin-screw extruder with a barrel temperature of 160–190 °C. After palletized and dried, blends were injected into a mold with the aid of a SZ 100 g injection-molding machine with a barrel temperature of 190 °C and an injection pressure of 900 kg/cm^2. Then dynamic packing injection molding (DPIM) technology was applied. The schematic diagram of DPIM device is shown in Fig. 1. The shear stress field was introduced to the cooling melt during packing stage by two pistons that moved reversibly with the same frequency. Thus, a sample with highly oriented structure was generally obtained in this way. In our experiment, the injection molding under static packing was also carried out by using the same processing parameters but without shear for comparison purpose. The specimen obtained by dynamic packing injection molding is called dynamic sample, while the specimen obtained without shear is called static one.

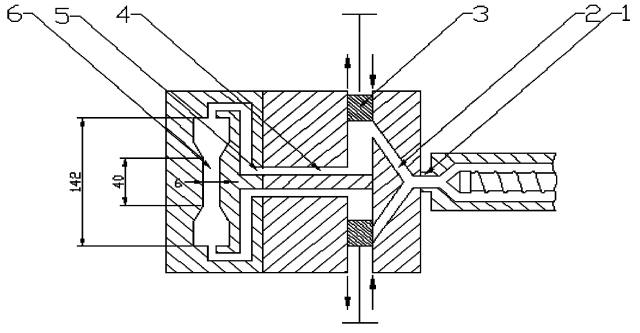

Fig. 1. Schematic diagram of the device for dynamic packing injection molding. (1) Nozzle, (2) sprue, (3) piston, (4) runner, (5) connector, (6) specimen.

2.2. SEM observation

The specimen was first etched by 1% solution of potassium permanganate in a mixture of sulphuric acid, 85% orthophosphoric acid and water [23], then the surface was coated with gold and examined by an X-650 Hitachi scanning electron microscope at 20 kV.

2.3. 2D-WAXS measurement

The two-dimensional wide-angle X-ray scattering (2D-WAXS) experiments were conducted using a Rigaku Denki RAD-B diffractometer. The wavelength of the monochromated X-ray from Cu Kα radiation was 0.154 nm and reflection mode was used. The intensity was corrected by subtracting the background scattering. The orientation of chains could be quantified by the orientation factor f

$$f = \frac{3\langle\cos^2\theta\rangle - 1}{2} \tag{1}$$

$$\langle\cos^2\theta\rangle = \frac{\int_0^{\pi/2} I(\phi)\sin\phi\cos^2\phi \mathrm{d}\phi}{\int_0^{\pi/2} I(\phi)\sin\phi \mathrm{d}\phi} \tag{2}$$

θ is the angel between the normal of a given (*hkl*) crystal plane and shear flow direction, and I is the intensity. When taking $\theta = 0$ as the shear flow direction, f is -0.5 for a perfect perpendicular orientation and $+1.0$ for a perfect parallel orientation; f equals 0 for an un-oriented sample.

2.4. Ultrasonic detection

The ultrasonic system used in the experiment was described elsewhere [24] except that the pulsing/receiving transducer consisted of normal incident shear wave transducer with a frequency of 5 MHz, which was purchased from Panametrics Inc. When propagating in anisotropic media

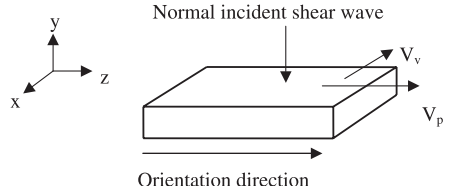

Fig. 2. Schematic diagram of normal incident shear wave propagation in uni-oriented media.

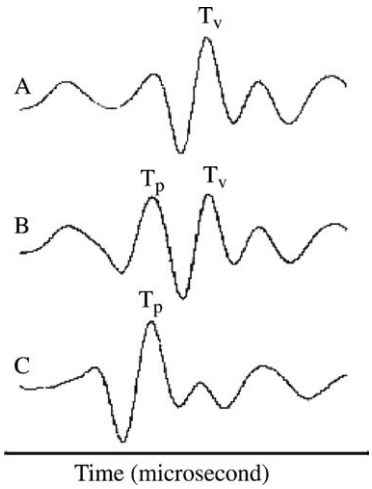

Fig. 3. Echo signals of normal incident shear wave with particle displacement (A) vertical, (B) 45° or (C) parallel to orientation direction.

(uniaxial orientation) along y direction, shear wave has two characteristic velocities, depending on the direction of the particle displacement vector (Fig. 2). The shear wave velocity is V_p when the particle displacement vector is in the z direction (parallel to the orientation direction), and V_v when in the x direction (vertical to the orientation direction). Correspondingly, V_p, V_v can be formulated as

$$V_p = \sqrt{\frac{c_{xz}}{\rho}} \tag{3}$$

$$V_v = \sqrt{\frac{c_{xy}}{\rho}} \tag{4}$$

where c_{xz} and c_{xy} refer to the shear stiffness in xz and xy plane, respectively. As far as oriented sample is concerned, the shear stiffness is different. Generally, the higher the orientation, the greater the difference in the shear stiffness is, consequently, the velocity difference between V_p and V_v is much higher. Therefore, the velocity difference ($V_p - V_v$) can be utilized to characterize the degree of polymer chain orientation.

Practically, the corresponding echo time is more convenient than velocity to reflect the orientation. Fig. 3 shows the echo signals of shear wave in oriented media. Curves A and C are the echo signals with particle displacement vertical and parallel to orientation direction, respectively, where T_v and T_p are the corresponding echo time. It is easily inferred that higher velocity results in shorter echo time, therefore, the difference in echo time $\Delta T = (T_v - T_p)$ can also characterize the degree of anisotropy. Similarly, larger difference in echo time $\Delta T = (T_v - T_p)$ corresponds to higher orientation. While the particle displacement is 45° to orientation direction, shear wave can travel in both characteristic velocity V_p and V_v simultaneously, so, the echo signal can also be divided into two echo time T_v, T_p (Fig. 3(B)). This property provides possibility using shear wave to monitor at real time the variation of oriented structure during processing through observing the two echo time T_v, T_p from the same echo signal.

3. Results

3.1. Orientation as detected by ultrasonic property

As for polymer blends, especially crystalline HDPE/*i*PP blends, the ultrasonic signals are complicated, compared with single phase polymer such as LDPE. As shown in Fig. 4, the shear wave travels in higher velocity when particle displacement parallel to flow direction than vertical to flow direction for HDPE/*i*PP (10:90) blends, $V_p > V_v$, accordingly, $T_v > T_p$, and the time difference $\Delta T = (T_v - T_p)$ is positive, similar to the ultrasonic results of LDPE in Edwards' work. In our experiment, it is found that $\Delta T = (T_v - T_p)$ always keeps positive when *i*PP content is more than 50 vol%. However, as *i*PP content is less than 50 vol%, contrary phenomena is observed, namely, the velocity with particle displacement parallel to flow direction is lower than that vertical to flow direction ($V_p < V_v$) and $\Delta T = (T_v - T_p)$ becomes negative (Fig. 5). Since, the phase morphology has a great effect on the ultrasonic property, the SEM experiment was carried out to examine the phase morphology. This is shown in Fig. 6. Due to its poorer resistibility to the etchant, *i*PP component was extracted from the samples, represented by the dark area in the pictures. One observes a co-continuous morphology around the composition of 50 vol% *i*PP, and a sea-island structure at 20 vol% *i*PP and 70 vol% *i*PP. That is to say, when *i*PP content is lower than 50 vol%, HDPE forms the continuous phase and *i*PP forms the dispersed phase, and higher than that composition, *i*PP becomes the continuous phase and HDPE forms the dispersed phase. It seems that the ultrasonic behavior is closely related to the major component in HDPE/*i*PP blends.

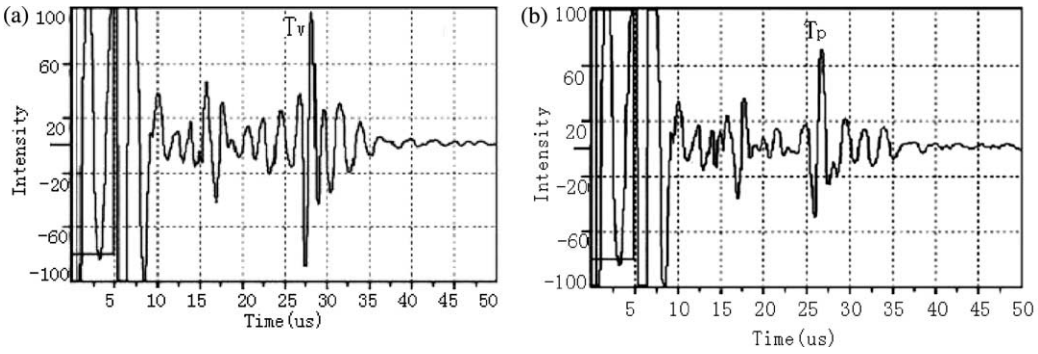

Fig. 4. Echo signals of HDPE/*i*PP (10:90) dynamic sample with particle displacement (a) vertical and (b) parallel to flow direction.

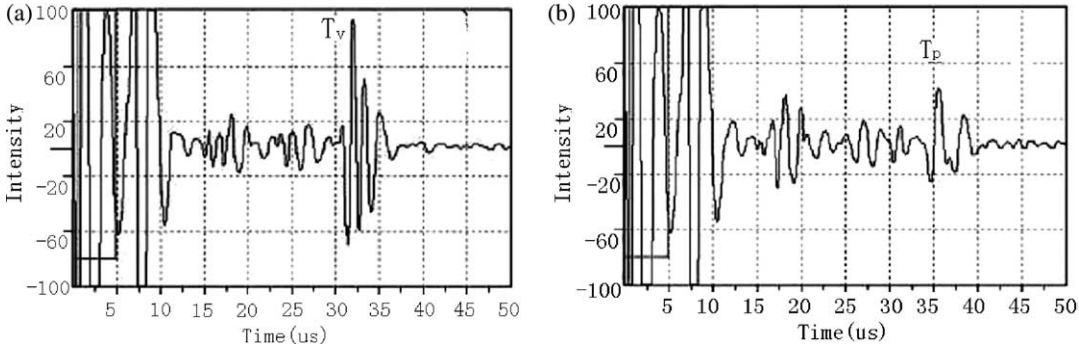

Fig. 5. Echo signals of HDPE/*i*PP (70:30) dynamic sample with particle displacement (a) vertical and (b) parallel to flow direction.

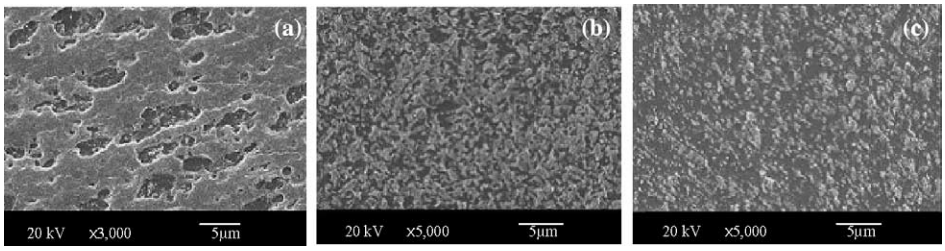

Fig. 6. SEM pictures of dynamic samples perpendicular to flow direction with different composition, (a) HDPE/*i*PP (80:20), (b) HDPE/*i*PP (50:50) and (c) HDPE/*i*PP (30:70).

The different phenomena may be caused by the change of shear stiffness due to the phase inversion, and will be discussed later. According to Eqs. (3) and (4), however, disregarding V_p is higher than V_v or not, the high orientation usually leads to high anisotropy in velocity. Therefore, the difference between two, or the absolute value of $\Delta T = (T_v - T_p)$ can be used to check the degree of orientation in the samples.

Fig. 7 shows the echo time difference for HDPE/*i*PP blends as a function of composition, where, the time difference is divided by the thickness of individual sample along the propagation direction in order to avoid the error arising from the thickness difference. It can be seen that the echo time difference of polymer blends is related to its composition and processing method. For static samples, one observes a very low time difference (within 0.04 μs/mm) in the whole composition region and this can be understood as due to almost isotropic structure in these samples. For dynamic samples, an oriented structure is expected. One observes a big time difference when *i*PP content is less than 50 vol%, and the time difference increases with decreasing of *i*PP content (reaches to 0.12 μs/mm). This result suggests that a highly oriented structure may exist when HDPE is dominant and forms the continuous phase, and the degree of orientation increases with decreasing of *i*PP content. On the other hand, when *i*PP content is more than 50 vol%, i.e. *i*PP is dominant and forms the continuous phase, one observes a constant echo time difference (roughly 0.05 μs/mm) as change of composition. This indicates that once *i*PP forms the continuous phase the orientation will keep unchanged with the change of composition. But the small echo time difference suggests a limited orientation in this case.

In summary, by measuring the echo time difference between vertical and parallel to the shear flow direction, one can easily know the orientation in the obtained samples obtained by either static packing injection molding or dynamic packing injection molding. For static samples, not much orientation is achieved; for dynamic samples, a highly oriented structure is achieved when HDPE forms the continuous phase, but only a limited orientation is obtained when *i*PP forms the continuous phase. This result is within our expectation and understood as due to the linear structure of HDPE and the hindrance effect of $-CH_3$ group on the *i*PP orientation.

3.2. Orientation as verified by 2D-WAXS

To better understand and verify the orientation structure in HDPE/*i*PP blends, powerful 2D-WAXS was employed to explore the orientation state of polymer chains in each

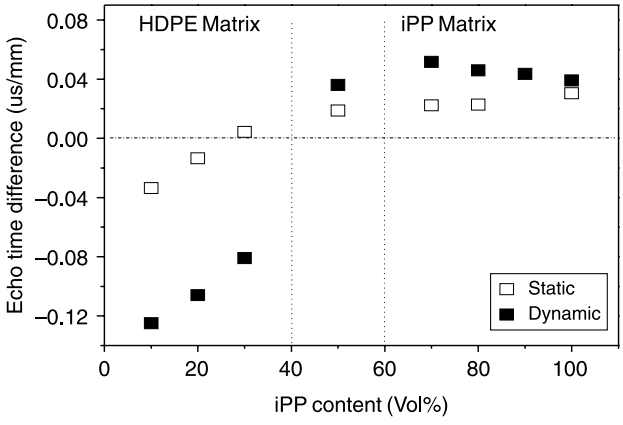

Fig. 7. Echo time difference between T_v and T_p as a function of *i*PP volume fraction for HDPE/*i*PP samples.

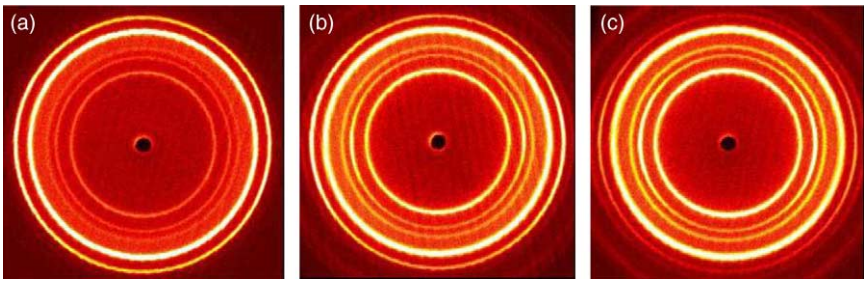

Fig. 8. 2D-WAXS patterns of static samples. (a) 20 vol% *i*PP, (b) 50 vol% *i*PP and (c) 80 vol% *i*PP. Flow direction is vertical.

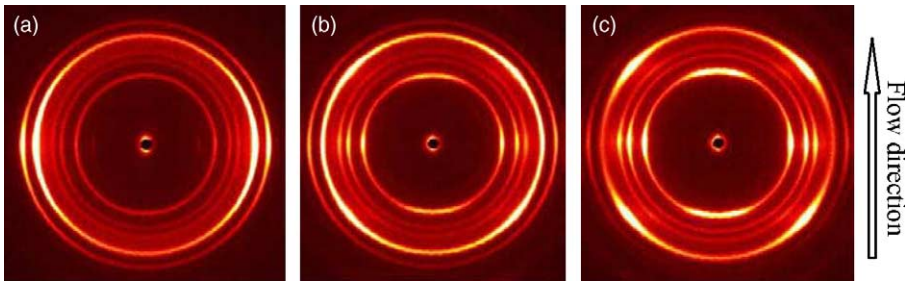

Fig. 9. 2D-WAXS patterns of dynamic samples. (a) 20 vol% *i*PP, (b) 50 vol% *i*PP and (c) 80 vol% *i*PP. Flow direction is vertical.

component. The 2D-WAXS patterns of static samples are shown in Fig. 8. From inner outward, the reflections are originated from (110), (040), (130) plane of alpha modification of *i*PP and (110), (200) plane of orthorhombic modification of HDPE. These homocentric circles imply that either HDPE chains or *i*PP chains are oriented randomly over the all ranges of composition.

However, as for dynamic samples, strong reflections of (*hk*0) plane for *i*PP component at the equator indicate that molecular chains of *i*PP are preferentially oriented along flow direction, independent of compositions (Fig. 9). Four reflections around the meridian also emerge in the (110) plane of *i*PP, especially between the compositions of 50 and 80 vol% *i*PP, indicating a lamellar branching through homoepitaxy between α-crystals of *i*PP [25,26]. These arise from the *i*PP component daughter lamellar regions (*a*-axis parallel to the meridional direction) and related to the *i*PP parent lamellar regions (*c*-axis parallel to the meridian). The epitaxial orientation relationship was first established in α-crystal quadrate some years ago and later explained on a molecular basis by Lotz et al. [25]. In daughter lamella, the molecular chains are oriented perpendicular to flow direction.

As for HDPE component, it can be seen from Fig. 9 that the reflections of both (110) and (200) plane of HDPE at the composition of 20 vol% *i*PP occur at the equator, indicating that HDPE chains are oriented along flow direction, with lamella perpendicular to flow direction [27]. But in the compositions of 50 and 80 vol% *i*PP, four reflection spots are always observed 50° apart from the meridian. Combining the permanent equatorial reflection of (200) plane, this special reflection can be ascribed to the epitaxial growth of HDPE lamella onto that of *i*PP, since HDPE chains are inclined about 50° to the *i*PP chain axis and the contact plane is established to be (100) of HDPE and (010) of *i*PP [28].

The orientation factor of the normal of given crystal planes, with respect to the shear direction, is shown in Fig. 10, including both dynamic and static samples. As for (110) plane of HDPE, the orientation factor in dynamic samples varies with phase morphology. Its value is about 0 when HDPE forms the dispersed phase in its droplets with *i*PP content between 50 and

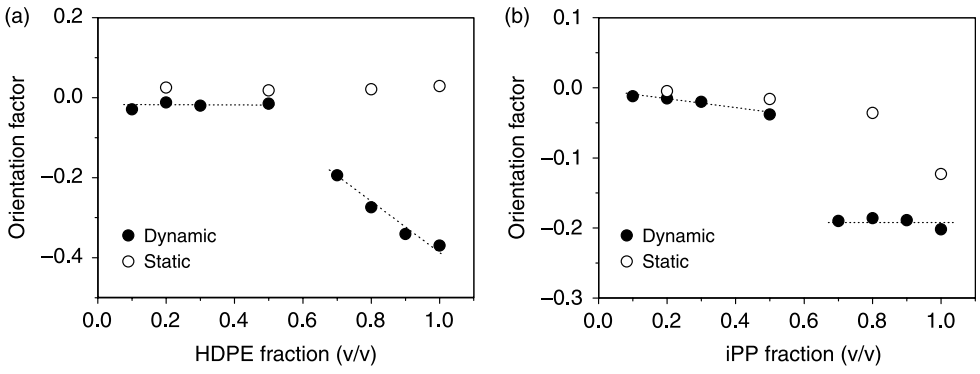

Fig. 10. Orientation factor of (110) plane of HDPE (a) and (040) plane of *i*PP (b) for both dynamic and static samples, with respect to compositions.

80 vol%, which originates from the special angle (~50°) between the normal and shear direction due to epitaxial growth. However, when HDPE forms the continuous phase as a matrix, the orientation factor drops down to −0.2 to −0.4 with reducing *i*PP content in its matrix, indicating a higher molecular orientation along flow direction. The orientation factor of static samples is close to 0 in all compositions for (110) plane of HDPE, indicating a random orientation. Similar to that of HDPE, the orientation factor of (040) plane of *i*PP in dynamic samples is also different in its matrix and droplets. When dispersed in the HDPE matrix, the value decreases slightly down to about −0.05. When *i*PP forms continuous phase, however, the orientation factor keeps unchanged around −0.2. As for static samples, the orientation factor of (040) plane is decreased down to roughly −0.1 when *i*PP content is up to 100%. This increased orientation in static sample may be related to flow-induced crysallization [29,30]. It can be also safely concluded that the change of molecular chain orientation in their individual matrix is more obvious for HDPE than for *i*PP, again due to the linear structure of HDPE. The 2D-WAXS result is consistent with the ultrasonic data.

4. Discussion

Now it is clear that the orientation in HDPE/*i*PP blends obtained by injection molding can be well characterized by measuring the ultrasonic property and verified by the well-established technique 2D-WAXS. That is, when HDPE forms the matrix, HDPE chains are oriented along flow direction and when *i*PP forms the matrix, *i*PP chains in parent lamella are oriented along flow direction while chains in daughter lamella are perpendicular to flow direction. The remaining question is how we understand that V_p is always lower than V_v in oriented HDPE matrix, which is contrary to the propagation behavior in oriented LDPE sample [19]. A very low crystallinity and orientation exists in oriented LDPE due to its highly branched structure. Thus, a few lamella stacks are oriented vertical to the flow direction. So, V_p is higher than V_v in oriented LDPE. For oriented HDPE matrix, however, highly oriented stacks exist vertical to the flow direction with the molecular orientation along flow direction. It seems that shear wave travels faster with particle displacement along lamella direction than along molecular chain direction in crystalline polymer. This may explain in part that V_p is always lower than V_v in oriented HDPE matrix. However, for oriented *i*PP matrix, parent lamella (vertical to flow direction) and daughter lamella (parallel to flow direction) co-exist along different direction in *i*PP phase. Herein, daughter lamella may be dominant to govern the shear wave propagation, thus, velocity with particle displacement parallel to flow direction keeps higher than that perpendicular to flow direction in *i*PP matrix. Above all, the velocity should finally be governed by corresponding shear stiffness, but how the shear stiffness varies with composition in HDPE/*i*PP blends will be investigated further.

The comparison of ultrasonic results and 2D-WAXS results is shown in Fig. 11, where all the negative echo time difference switches to positive one for the purpose of comparison, in that

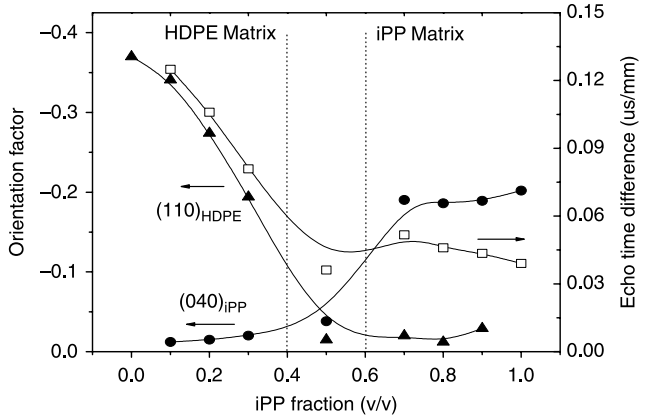

Fig. 11. Comparison of ultrasonic results and 2D-WAXS results in terms of orientation measurement for HDPE/*i*PP blends.

the orientation degree is only related to the absolute value of echo time difference. These two methods adopt two different parameters to describing the orientation structure: orientation factor f for 2D-WAXS, and echo time difference ΔT for ultrasonic method. So, only the trend of orientation variation with composition, and the relative ratio of orientation between HDPE and *i*PP matrix make sense. It can be seen that whenever in HDPE matrix or *i*PP matrix, the variation of echo time difference with composition is always similar to that of orientation factor for major component, especially in the HDPE matrix. It implies that the overall orientation state is dominated by the major component. Meanwhile, it is also shown in Fig. 11 that the ratio of orientation between the HDPE matrix and the *i*PP matrix for ultrasonic results is higher than that for 2D-WAXS results. This probably results from the fact that 2D-WAXS only measures the orientation of molecular chain in parent lamella according to the reflection of (040) plane at the equator for *i*PP component, whereas, ultrasonic method concerns the overall orientation based on the anisotropy in shear stiffness, which would be weakened by the co-existence of parent and daughter lamella vertical to each other.

5. Conclusion

According to the property that ultrasound travels in different velocities in anisotropic media, normal incident shear wave was utilized to explore the orientation structure of HDPE/*i*PP blends obtained by dynamic packing injection molding. It reveals that the HDPE component is more apt to orient than *i*PP component in shear stress field, and the overall orientation of blends is dominated by the major component whenever in HDPE or *i*PP matrix. The ultrasonic technique is consistent with the 2D-WAXS in charactering the orientation degree of polymer chains, although ultrasonic technique focuses on the overall orientation of polymer blends while the 2D-WAXS reveals the crystalline orientation of each component. Our work demonstrates that ultrasonic technique might be a reliable, fast and easy way to characterize the orientation structure of polymer, and provides the possibility for real time

detection of orientation structure in injection molding by using ultrasonic technique.

Acknowledgements

We would like to express our great thanks to the National Natural Science Foundation of China for Financial Support (20404008, 50373030 and 50533050). This work was subsidized by the Special Funds for Major State Basic Research Projects of China (2003CB615600) and by Ministry of Education of China as a key project (104154).

References

[1] Odell JA, Grubb DT, Keller A. Polymer 1978;19:617.
[2] Keller A. Polymer 1962;3:293.
[3] Bafna A, Beaucage G, Mirabella F, Mehta S. Polymer 2003;44:1103–15.
[4] Na B, Wang Y, Zhang Q, Fu Q. Polymer 2004;45:6245–60.
[5] Zhu L, Calhoun BH, Ge Q, Quirk RP, Cheng SZD, Thomas EL, et al. Macromolecules 2001;34(5):1244–51.
[6] Fakirov S, Stribeck N, Apostolov AA, Denchev Z, Krasteva B, Evstatiev M, et al. J Macromol Sci, Phys 2001;B40(5):935–57.
[7] Wu J, Schultz JM. Polymer 2002;43:6695–700.
[8] Carbonnier B, Andreopoulou AK, Pakula T, Kallitsis JK. Macromol Chem Phys 2005;206(1):66–76.
[9] Bubeck RA, Thomas LS, Rendon S, Burghardt WR, Hexemer A, Fischer DA. J Appl Polym Sci 2005;(98):2473–80.
[10] Wang Y, Na B, Fu Q, Men YF. Polymer 2004;45:207–15.
[11] Fujiyama M, Wakino T. J Polym Sci 1991;42:9.
[12] Kantz MR, Newman HD. J Appl Polym Sci 1972;16:1249.
[13] Shigemitsu M, Yoshiyuki N, Masahide Y. Polymer 1997;38(18): 4577–85.
[14] Sakata J. Thin Solid Films 1998;333(1–2):213–8.
[15] Mendoza R, Regnier G, Seiler W, Lebrun JL. Polymer 2003;44(11): 3363–73.
[16] Cole KC, Ben DH, Sanschagrin B, Bguyen KT, Ajji A. Polymer 1999; 40(12):3505–13.
[17] Binder H, Kohlstrunk B. Vib Spectrosc 1999;21(1–2):75–95.
[18] Lapersonne P, Bower DI, Ward IM. Polymer 1992;33(6):1266–76.
[19] Edwards R, Thomas C. Polym Eng Sci 2001;41(9):1644–53.
[20] Wang Y, Na B, Fu Q. Chin J Polym Sci 2005;23(1):103–11.
[21] Na B, Zhang Q, Wang Y, Fu Q. Polym Int 2004;53(8):1078–86.
[22] Zhang Q, Wang Y, Fu Q. J Polym Sci, Part B: Polym Phys 2003;41(1): 1–10.
[23] Olley RH, Bassett DC. Polymer 1982;23:1707.
[24] He BB, Yang Y, Zou H, Zhang Q, Fu Q. Polymer 2005;46:7624–31.
[25] Lotz B, Wittmann JC. J Polym Sci, Part B 1986;24:1559.
[26] Padden FJ, Keith HD. J Appl Phys 1973;44:1217.
[27] Na B, Wang K, Zhao P, Zhang Q, Du RN, Fu Q. Polymer 2005;46: 5258–67.
[28] Yan S, Petermann J, Yang D. Polymer 1998;39:4569.
[29] Somani RH, Hsiao S, Yang L. Macromolecules 2002;35:9096.
[30] Pogodina NV, Lavrenko VP, Winter HH. Polymer 2001;42:9031.